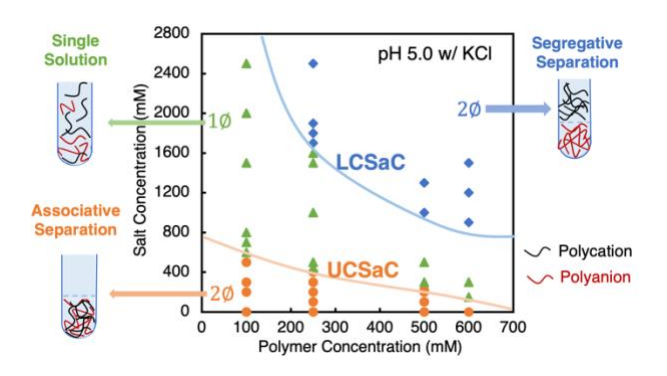
Salt-Dependent Phase Re-entry of Weak Polyelectrolyte Complexes: from Associative to Segregative Liquid-Liquid Phase Separation

Huiling Li¹, Ying Liu¹, Fujie Lan², Mohsen Ghasemi², Ronald G. Larson^{1,2}*

¹ Macromolecular Science and Engineering Program, University of Michigan, Ann Arbor, Michigan 48109

² Department of Chemical Engineering, University of Michigan, Ann Arbor, Michigan 48109 *Corresponding author E-mail: rlarson@umich.edu



For Table of Contents use only

ABSTRACT

A high-salt phase-separation re-entry is observed in mixtures of poly (diallyldimethyl ammonium chloride) (PDADMAC), a strong polycation, and poly (acrylic acid) (PAA), a partially charged

polyanion, within the pH range 4.7 to 5.3. This intriguing phenomenon exclusively occurs at salt concentrations exceeding the critical salt concentration required for dissolving the coacervate formed at low salt concentrations, here named the "Upper Critical Salt Concentration" (UCSaC), and at monomer concentrations exceeding 0.1M for each polymer. The transition from associative phase separation at low salt concentration, to a single solution, and ultimately to segregative separation at high salt concentration called the Lower Critical Salt Concentration (LCSaC), arises from the interplay between electrostatic interactions and the hydrophobicity of neutral PAA monomers in a high-salt solvent. To explain this transition, we use a theory combining short-range ion pairing and counterion condensation with long-range electrostatics using the random phase approximation (RPA), and with hydrophobic interactions between PAA neutral monomers and water. The latter is modeled through a Flory-Huggins χ parameter of around 0.6. Literature observations of a continuous transition from associative to segregative phase transition with increasing salt concentration, without a homogeneous single-phase solution at intermediate salt concentration, are also predicted and discussed.

1. INTRODUCTION

Liquid-liquid phase separation of oppositely charged polyelectrolytes (PE's), often called coacervation, occurs not only in commercial products, such as food emulsifiers, hampoos, bio-based coatings for packaging applications, and water-treatment materials, but also plays essential roles in biology, including the formation of membraneless organelles, protein aggregation, peptide delivery, DNA packaging, and viral assembly. While the mixing of solutions of two neutral polymers often leads to a *segregative* phase separation in which the two different polymers are separated into distinct phases, the formation of polyelectrolyte coacervates is often through an

associative phase separation, since oppositely charged polyelectrolytes often attract each other and phase separate into a dense coacervate. The addition of salts weakens association of the oppositely charged polymers, often increasing its phase volume due to hydration, similar to the response of biological membranes to increases in salt concentration.

There have been significant efforts to develop a comprehensive theory to predict the phase behavior of these complex systems, starting with the Voorn-Overbeek (V-O) theory from the 1950's.⁽⁷⁾ This early approach combines conventional Flory-Huggins⁽⁸⁾⁽⁹⁾ theory for the entropy of mixing with the Debye-Huckel theory(10) for the electrostatic free energy, but neglects the connectivity of the polymeric charges and the effects of short-range electrostatic interaction. The importance of non-electrostatic interactions contained in the Flory-Huggins χ parameter was demonstrated in experiments showing a heat of mixing in coacervation of protein polyelectrolytes mixtures motivating extension of the V-O theory to include a χ parameter. While good fits of the extended V-O theory with experimental data have been shown, (12) this success is likely due to the liberal use of fitting parameters to counteract the neglect of charge connectivity, short-range electrostatic interaction, charge density fluctuations, and other effects from the V-O theory. To account for charge connectivity, the random phase approximation (RPA) has been employed, (13)-(15) while short-range electrostatic interactions have been modeled through phenomenological reversible ion-pairing reactions and counterion condensation. (16)-(24) (We note, however, that for strongly charged densely packed polymers, the suitability of representing local charge interactions as ion pairs has been questioned, and other approaches to strong ion correlations have been proposed. (24) Numerous other approaches have emerged to address the limitations of the original V-O theory, including liquid state theories, (25)-(27) scaling theories, (28)-(30) and field theoretic

simulations.⁽³¹⁾⁽³²⁾ These approaches have been developed as complementary methods to overcome the deficiencies of the V-O theory. Recent reviews have provided comprehensive summaries and comparisons of the advancements made in polyelectrolyte theory.⁽³³⁾⁻⁽³⁵⁾

Despite the various advances, most modeling has been restricted to strong polyelectrolytes with a fixed extent of charge. However, for weak PE the charge density changes in response to the environment, especially to pH. (36) This phenomenon, known as charge regulation, when incorporated into theories, (22),(36) is found to be influenced by counterion condensation, and is dependent on the physico-chemical properties of the charged groups, often quantified by a binding free energy. (21) The Larson group established a thermodynamic model that incorporates charge regulation, electrostatic interactions, and binding between small ions and polymer ions, treated as reversible chemical reactions. (22) This theory, which used the Voorn-Overbeek expression for electrostatic free energy, was later extended to include polymer charge connectivity using the random phase approximation (RPA) in collaboration with the Qin group. (17) It was then used to explore phase behavior of two oppositely charged strong polyelectrolytes (37)(38) and charge regulation of a single weak polyelectrolyte. (36) However, this theory containing RPA has not yet been extended to include charge regulation when there two oppositely charged polymers. Moreover, none of these theories include correlations of charge along the backbone of a weak polyelectrolyte, a limitation addressed by the transfer matrix approach of Sing and coworkers. (39) Since our current model for oppositely charged polyelectrolytes does not include charge regulation, we will model qualitatively the effect of pH by imposing a fixed fractional charge on the weak polyelectrolyte to reflect the pH at which the experiments were conducted, with higher fractional charge corresponding to a higher pH, as discussed in what follows.

To test the success of such improvements in modeling, it is important that comparisons can be made with experimental data, for example with experimental phase diagrams, including the phase boundary and phase compositions. To identify the conditions under which mixtures of polyelectrolyte solutions will form distinct phases or remain a single phase, experimental researchers have used techniques such as visual observation, turbidometry, micrometry, UV spectrometry, and conductometry. (40)(48) Additionally, thermal gravimetric analysis (TGA)(41) can be used to quantify the total polymer composition, while nuclear magnetic resonance (NMR)(44)(47),(48) or fluorescence correlation spectroscopy (FCS)(12) can be used to determine the compositions of individual polymers. A general analytical protocol has been put forwarded to help standardize the experimental quantification of polyelectrolyte coacervates. (42)

While many theories and experimental studies^{(49),(50)} have been conducted on polyelectrolyte complexes (PECs), few have focused specifically on weak PE's. While PECs made of either weak or strong PE's are sensitive to the concentration and identity of added salts, polymer concentration and chain length, PECs with at least one weak PE are also sensitive to solution pH. Jha and coworkers used an "extended" V-O theory that included charge regulation by an experimentally guided ad hoc pH-dependent degree of polyelectrolyte charge. With this they predicted a "segregative" phase separation in which cationic poly (diallyl dimethyl ammonium chloride) (PDADMAC) and anionic poly (acrylic acid) (PAA) appear in separate phases at pH 4.⁽⁴³⁾ Tirrell and coworkers⁽⁴⁴⁾ have reported experimentally a continuous phase transition from associative separation to segregative separation in weak polyelectrolyte complexes of poly (acrylic acid) (PAA) and poly (allylamine hydro-chloride) (PAH). Li et al.⁽⁴⁵⁾ have studied the effect of solvent quality

on phase behavior in mixtures containing a weak polyelectrolyte and predicted a robust two-phase system even at very high salt concentration in poor solvents.

Building on this prior work, we here study systematically the phase behavior of mixtures of oppositely charged polyelectrolytes with one of them weak, specifically focusing on PDADMAC/PAA, while considering a range of parameters such as pH, salt identity and concentration. To differentiate associative from segregative phase separation, carbon-13 NMR techniques is employed to indicate whether the two polymers are predominantly in the same or different phases. A previously developed thermodynamic model is applied to predict and explain the physical properties and phase transitions observed in the experiments. The concepts of lower critical salt concentration, named LCSaC, and upper critical salt concentration, named UCSaC, are put forward to describe the effect of salt concentration on phase transitions.

2. METHODS

2.1 EXPERIMENTS

Polyelectrolyte complexes samples were prepared by mixing separately prepared stock solutions of polycation, polyanion, and salt with designed concentrations at different ratios of volumes. Firstly, a solution of poly (acrylic acid) (35 wt% in water) with a molecular weight of 100,000 g/mol and of poly (diallyl dimethylammonium chloride) (35 wt% in water) with a molecular weight less than 100,000 g/mol, purchased from Sigma-Aldrich, were diluted to stock solutions with an overall monomer concentration of 2M. Crystalline NaCl and KCl (Sigma-Aldrich) were each dissolved in Milli-Q purified water (Thermo Scientific, MicroPure UV/UF) with a resistivity of 18.1 M Ω cm at 24 \pm 1°C to prepare 4M salt stock solutions. Second, the pH of the PAA stock

solutions were adjusted from their original value of 1.6 to approximately 4.7, 5.0, 5.2, and 7 by adding solid NaOH or KOH pellets (Sigma-Aldrich), depending on the salt identities used in the final mixtures. The original pH of PDADMAC stock solutions was around 4.8, and it was left unadjusted since its contribution to the pH of the final mixture was deemed insignificant. (It was determined that the pH value of the final samples was primarily influenced by the weak polyanion present in this system.) Then, appropriate volumes of PDADMAC and PAA stock solutions (with the designated pH) were added to a centrifuge tube containing a pre-calculated volume of salt stock solution and ultrapure water. For example, a sample with a total volume of 4.8ml and a monomer concentration of 0.5M of each polymer at a final added salt concentration of 1M is made by mixing 1.2ml of PDADMAC stock solution of 2M monomer concentration, 1.2ml of PAA stock solution of 2M monomer concentration, 1.2ml of KCl solution of 4M concentration, as well as 1.2ml of ultrapure water. The samples were vortexed and well mixed between each addition of stock solution and centrifuged for 5 minutes at 5000 rpm (MTC Bio MyFuge) as the final step of preparation. All samples were left undisturbed for at least five days until there were no changes in phase separation or appearance. The volume of upper liquid-like phase (supernatant) for phase separated samples was recorded by pipette during transfer, and then the volume of the lower phase (coacervate) was obtained by subtracting the volume of upper phase from the total known volume.

To determine the composition of each phase, the separated lower and upper phases were dried at 110°C for at least 24 hours until the remaining mass was constant. To dissolve the solid samples, deuterated oxide (Acros Organics) was added, which reduced the interference from non-deuterium solvents during NMR tests. In some cases, extra crystalline salts were added to help the solid polyelectrolytes redissolve. The redissolved samples in deuterated oxide solution were then

transferred to 5mm NMR tubes (Wilmad LabGlass) and measured by Carbon NMR (Varian MR400) from 0 to 200 ppm with 1000 scans and a 1s delay time, following a previous protocol⁽⁴²⁾ for measuring PDADMAC and PAA polyelectrolytes.

Single PAA samples with varying salt concentrations were prepared similarly by mixing 2M PAA stock solutions (pH 5 and pH 7, molecular weight 100KDa) with 4M salt stock solutions and water at different volume ratios to achieve the overall added salt concentrations ranging from 0 to 3.8M and monomer concentrations of 0.1M, 0.25M, and 0.5M.

2.2 THERMODYNAMIC MODEL

We employ a theoretical framework initially developed by Salehi and Larson⁽²²⁾ that integrated charge regulation and ion binding into an extended Voorn-Overbeek theory of Jha et al., ⁽⁴³⁾ and to which charge connectivity effects were added through the random phase approximation (RPA) by Friedowitz et al. ⁽¹⁷⁾ This theory was subsequently applied by Ghasemi and Larson^{(37),(38)} to understand overcharging and salt doping in strong polyelectrolyte complexes. Here, we adapt this theory ^{(37),(38)} to coacervation involving a weak polyelectrolyte, similar to our experimental system PDADMAC/PAA with KCl or NaCl, that includes a partially charged polyanion, a fully charged polycation, and added salt. The Helmholtz free energy density of each phase is calculated using closed-form contributions from the translational entropy of all species f^T , non-electrostatic interactions between polyions and solvent f^{χ} , long range electrostatic interactions based on the RPA $f^{corr,RPA}$, local ion-binding free energies among charged macroions and small ions f^{rxn} , and combinatorial binding entropy of charged polymers f^{comb} , as shown in equation (1). Since a detailed description of this theory can be found in previous work, ^{(22),(37),(38)} we here provide only a

basic explanation of the concepts and how the theory is applied to compare to our experimental data.

$$f = f^{T} + f^{\chi} + f^{corr,RPA} + f^{rxn} + f^{comb}$$
 (1)

In equation (1), the first two contributions f^T and f^χ are obtained from Flory-Huggins theory.⁽⁵¹⁾ These contributions are given by equations (2) and (3), respectively, where A, C, +, -, w represent polyanion, polycation, small cation, small anion, and water, respectively. The ratio of the volume of molecular species i, which can be a monomer or a salt ion, to that of the water molecule is represented by ω_i so that $\omega_W = 1$ denotes the volume ratio of water to itself. ϕ_i is the volume fraction of species i and can be converted from the molar concentration in mM, c, using $\phi_i = \frac{18c_i\omega_i}{10^6}$. Here, N is the degree of polymerization, which is equal to 1 for salt and water. The Flory-Huggins interaction parameter, χ_{ij} , quantifies the non-electrostatic interaction energy between a pair of species, which here will include monomers of polyanion (A), polycation (C), and solvent (W), where we neglect such interactions involving salt ions.

$$f^{T} = \sum_{i=A,C,\pm,w} \frac{\phi_{i}}{\omega_{i} N_{i}} ln \phi_{i} \qquad (2)$$

$$f^{\chi} = \sum_{ij} \chi_{ij} \phi_i \phi_j = \chi_{AW} \phi_A \phi_W + \chi_{CW} \phi_C \phi_W + \chi_{AC} \phi_A \phi_C$$
 (3)

To account for polymer chain connectivity and conformation, a modified version of RPA has been incorporated into the theory by Qin and co-workers.⁽¹⁷⁾ This RPA is used to determine the long-range electrostatic correlation free energy, which is represented by equation (4). The square of the inverse screening length $\tilde{k}^2(q)$, which takes into account the chain structure, is controlled by the molecular size of each species, the radius of gyration of polymer, and the charge density of polyelectrolyte in the aqueous solution. The conformation of each polyelectrolyte is assumed to be Gaussian, in agreement with some neutron scattering experiments in dense coacervates, ⁽⁵²⁾ but

likely less valid in semi-dilute polyelectrolytes.⁽²⁸⁾ To clarify different choices of notation used by our group, the definitions of charge fractions of various polyelectrolyte systems in our previous theories are summarized in Table S1. Comparison between experimental data and the theory of Ghasemi et al.⁽³⁷⁾ with and without RPA (shown in Figure S1) has demonstrated the importance of inclusion of RPA to properly describe the phase behavior of polyelectrolyte complexes.

$$f^{corr,RPA} = \frac{1}{4\pi^2} \int_0^\infty q^2 \ln\left(1 + \frac{\tilde{\kappa}^2(q)}{q^2}\right) dq \qquad (4)$$

In an aqueous solution, monomers on a strong polyelectrolyte chain can exist in three typical states, including 1) a bare charged monomer, 2) a charged monomer bound by a salt ion, and 3) a charged monomer bound by an oppositely charged monomer. In this study, we treat these local salt ion bindings and monomer-monomer bindings as reversible chemical reactions, and the binding free energy can be expressed using equation (5), where α_{C-} , α_{A+} , β_{C} represent, respectively, the fraction of polycation monomers bound by a salt anion, the fraction of polyanion monomers paired by a salt cation, and the fraction of polycation monomers bound with a polyanion monomer. ΔG_{ij} denotes free energy of binding between species i and j and captures the ion-specific effects that depend on monomer chemical identity. (21)

$$f^{rxn} = \frac{\alpha_{C-}\phi_C}{\omega_C} \Delta G_{C-} + \frac{\alpha_{A+}\phi_A}{\omega_A} \Delta G_{A+} + \frac{\beta_C\phi_C}{\omega_C} \Delta G_{CA}$$
 (5)

The last free energy contribution in equation 1 is the combinatorial binding entropy, presented in equation (6), which considers the number of microstates with different distributions of unpaired monomers, monomers paired with salt ions, and monomer-monomer pairs along the polyelectrolyte backbone. β_A represents the fraction of polyanion monomers paired with polycation and is related to β_C through a stochiometric constraint of ion pairing leading to β_A =

$$f^{comb} = f_A^{comb} + f_C^{comb} + f_{CA-A}^{comb}$$

$$= \frac{\phi_A}{\omega_A} \left[\alpha_{A+} \ln \alpha_{A+} + \beta_A \ln \beta_A + (1 - \alpha_{A+} - \beta_A) \ln(1 - \alpha_{A+} - \beta_A) \right]$$

$$+ \frac{\phi_C}{\omega_C} \left[\alpha_{C-} \ln \alpha_{C-} + \beta_C \ln \beta_C + (1 - \alpha_{C-} - \beta_C) \ln(1 - \alpha_{C-} - \beta_C) \right]$$

$$- \frac{\phi_C}{\omega_C} \beta_C \ln \left[\frac{\phi_C}{\omega_C} \beta_C (\omega_A + \omega_C) \right]$$

$$(6)$$

To determine the equilibrium state of polyelectrolyte complexes containing two oppositely charged PE's, the free energy difference (f_{total}) between a free-energy-minimized phase-separated solution and a similarly minimized single-phase solution needs to be calculated numerically. This free energy difference is written in equation (7) where v is the volume fraction of the coacervate phase. If the total free energy of a free-energy-minimized coacervate/supernatant combination is lower by more than numerical error than that of a single solution, $f_{total_min} < 0$, then this system is expected to form two phases. Otherwise, a single solution is the more stable state for the polyelectrolyte mixtures. Note that the parameters describing the extents of ion binding, α_{C-} , α_{A+} , β_C , β_A , are self-consistently determined within each phase during the free energy minimization process, with the constraints of electroneutrality, incompressibility, and ion-pairing stoichiometry imposed on each phase. (22),(39) By setting the first derivative of equation (1) with respect to the three parameters, α_{C-} , α_{A+} and , β_{C-} equal to zero, three laws of mass action can be obtained for each phase, listed as equations (8-10). Here $\mu_{ij}^{corr,RPA} = \frac{\omega_i}{\phi_i} \frac{\partial f^{corr,RPA}}{\partial \xi_{ij}}$ ($\xi_{ij} = \alpha_{C-}$, α_{A+} , β_C) is the exchange chemical potential for ion association due to the long range electrostatic fluctuations. ϕ_+^f or ϕ_-^f denote the volume fractions of free cations and free anions in either coacervate or supernatant or single-phase solution.

$$f_{total} = ((1 - v) * f_{supernatant} + v * f_{coacervate}) - f_{bulk}$$
 (7)

$$\frac{\alpha_{A+}}{(1-\alpha_{A+}-\beta_{A})\phi_{+}^{f}} = exp\left[-\Delta G_{A+} - \mu_{A+}^{corr,RPA} + 1\right] \qquad (8)$$

$$\frac{\alpha_{C-}}{(1-\alpha_{C-}-\beta_{C})\phi_{-}^{f}} = exp\left[-\Delta G_{C-} - \mu_{C-}^{corr,RPA} + 1\right] \qquad (9)$$

$$\frac{\beta_{A} \omega_{C}}{(1-\alpha_{A+}-\beta_{A})(1-\alpha_{C-}-\beta_{C})\phi_{C}(\omega_{A}+\omega_{C})} = exp\left[-\Delta G_{CA} - \mu_{CA}^{corr,RPA} + 1\right] \qquad (10)$$

To simulate the experimental system PDADMAC/PAA with molecular weights of each PE around 100kDa, we choose appropriate input parameters listed in Table 1, including the bulk phase compositions such as monomer concentration (in mM) c_i , the degree of polymerization N_i , the relative molecular size ratio ω_i , as well as physical properties of polyelectrolytes, such as free energies of binding ΔG_{ij} (k_BT) and the Flory-Huggins parameters χ_{ij} . To focus on the effect of the non-electrostatic interactions between PAA and water, we keep the binding free energies $(\Delta G_{C-}, \Delta G_{A+}, \Delta G_{CA})$ and χ_{CW} constant in all systems, while χ_{AW} is adjusted to simulate different phase behaviors. The selection of the three ΔG values, representing various binding free energies, were for simplicity all taken to be -5 k_BT , a value within the range of literature-derived calculations from molecular dynamics simulations and fitting outcomes from experimental datasets. (21),(39) Considering the relatively favorable interaction between PDADMAC and water, χ_{CW} is fixed at 0.3. Since the parameter ΔG_{CA} accounts for interactions between the polycation and polyanion monomers, the dispersion interaction between these polyions is left out (i.e., $\chi_{AC}=0$) to avoid double counting the contributions from macroions. We have not attempted to account explicitly for likely reduction in dielectric constant due to concentration of hydrophobic polymer in the coacervate. However, in calculations using our theory we assume quite a strong free energy for binding of salt ions to charged monomers, namely $\Delta G = -5k_BT$, which might account indirectly for the strong salt ion binding that would result from a reduced dielectric constant. An explicit accounting for dependence of dielectric constant on polymer concentration, perhaps along the lines of the theory of Khoklov and coworkers, is worth considering in future work.

Since our computer code does not explicitly allow for uncharged monomers, a partially charged PAA is represented by renormalizing the "monomers" by lumping uncharged monomers into the charged ones. This reduces the number of renormalized monomers N_A per polyanion to the number of charged ones and reduces the PAA monomer molar concentration c_A to the concentration of charged monomers. To keep the polymer volume and coil size the same, this renormalization is done while maintaining unchanged the radius of gyration $R_{gA}^2 = \frac{N_A b^2}{6} \sim N_A \omega_A^{2/3}$ where b is the statistical segment length of the polyelectrolyte and overall volume fraction of the PAA in solution $(\phi_A \sim c_A \omega_A)$. These two constraints allow the two renormalized parameters N_A and ω_A to be calculated for partially charged chains, as shown in Table 1. Consequently, the charge level of the weak polyelectrolyte is lower than that of the fully charged one with the same polymer volume fraction but treating the partially charged polymer as fully charged within the code. We plan to introduce charge regulation into our model in the future to allow the charge level to adapt to the PH and composition through laws of mass action.

Table 1. Simulation Parameters

polyanion charge level	$c_A(mM)$	$c_C(mM)$	N_A	N_c	ω_A	$\omega_{\mathcal{C}}$	ω_S	$\Delta G(k_BT)$	Xcw	χ_{AW}]
------------------------	-----------	-----------	-------	-------	------------	------------------------	------------	------------------	-----	-------------	---

100%	10	00								
	200 250		1390	620	2.4					
	50	00								
	35%	35	100	695	620	6.8				
88		250								
176		500								
12.5%	13	100		620	19.2					
	31	250	348							
	62	500								

3. RESULTS AND DISCUSSION

3.1 ASSOCIATIVE PHASE SEPARATION

Liquid-liquid phase separation in solutions containing oppositely charged polyelectrolytes typically occurs at lower salt concentrations, reflecting the dominant role of short-range electrostatic interactions and the dissociation of counterions. The associative phase separation weakens with increasing salt concentration, eventually inducing a transition to a single phase as depicted in Figure 1. (Here the term "overall" is the concentration in the solution prior to phase separation.) Furthermore, experimental samples prepared by mixing highly charged PAA solutions at pH 7 with fully charged PDADMAC solutions at various polymer concentration have confirmed this transition, as shown in Figure 2.

Experimental and theoretical results in Figure 1(a) both show that an increase in monomer concentration leads to a higher volume fraction of coacervate and to a lower salt concentration for transition to a single phase, represented by the endpoint of the line. This suggests that for hydrophilic or highly charged polymers, polyelectrolyte complexes swell with added salt, ultimately transitioning to a single-phase solution. The shape of the coacervate volume fraction with added salt mimics that reported in our previous study. (39) The salt concentrations at the transition for monomer concentrations of 250 mM (red symbols) and 500 mM (green symbols) are approximately 290 mM and 25 mM, respectively. Taking into account counterions to the monomers, there are in total 540mM (250+290) and 525 mM (500+25) pairs of salt ions in these solutions, showing that as monomer concentration varies, the total concentration of salt ions necessary for the formation of a single-phase solution remains relatively constant, exceeding 500mM. Consequently, the high volume fraction of coacervate phase at high monomer concentration, surpassing 80% for 500mM polyelectrolyte concentration, can be attributed to the hydration of highly charged monomers and also to the large concentration of counterions in the coacervate, which weakens the association among monomers.

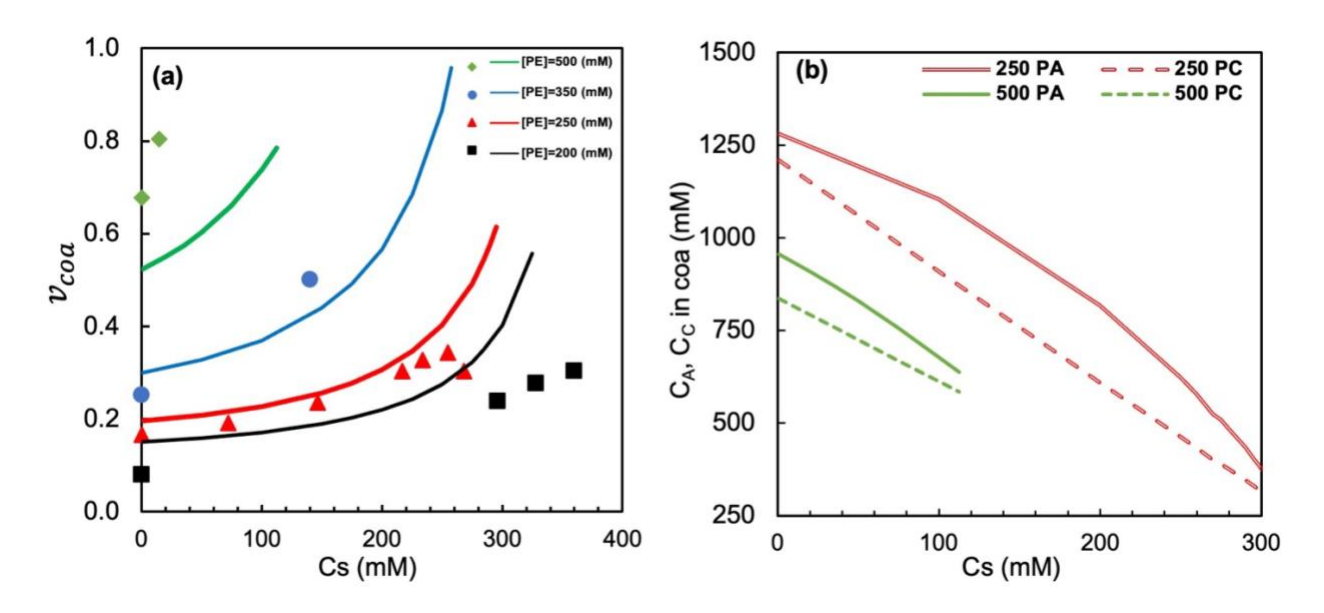


Figure 1. (a) Volume fraction of the coacervate phase, v_{coa} , as a function of added salt concentration, Cs, for a fully charged polyelectrolyte system of PDADMAC/PAA at pH 7 and various polymer concentrations, from experiments (symbols) and theory (solid lines). (b) Predicted polymer composition (polyanion denoted by PA and polycation by PC in the legend) in coacervate phase as a function of overall added salt concentration at overall monomer concentrations of 250mM and 500mM of each PE. Here $\chi_{AW} = 0.45$, with other parameters given in Table 1.

Figure 1(b) shows that both polyanions and polycations are present within the coacervate phase across all concentration ranges. However, the polyanion exhibits a slightly higher concentration than the polycation, even though an equal amount of both species were considered in the theoretical calculations. This difference in phase composition can be attributed to the different values of the Flory-Huggins parameters, namely $\chi_{AW}=0.45$ and $\chi_{CW}=0.30$, implying that the polyanion has less preference for water than does the polycation. Other theoretical parameters employed in these calculations in Figure 1, including degrees of polymerization N_A and N_C , monomer concentrations c_A and $c_{A'}$ relative molecular size ratio ω_A or ω_C , were chosen based on the experimental system

PDADMAC/PAA with 100kDa molecular weight and can be found in Table 1 for 100% charge level. In Figures 1 and 2, nearly all the polymer resides in the coacervate phase, as can be seen by multiplying the volume fraction of coacervate by the concentration of the polycation or polyanion within the coacervate. (For example, for 250mM total monomer concentration, Fig. 1(a) shows a predicted 0.2 volume fraction of coacervate at zero added salt, which, when multiplied by 1250mM PAA concentration in the coacervate phase shown in Fig. 1(b), gives back the overall concentration of 250 mM). For zero added salt, the polymer concentration within the coacervate is maximized due to the relatively small coacervate volume. As the coacervate swells in the presence of added salt, approaching the single-phase region, the polymer concentration in the coacervate decreases and converges towards that of the overall composition.

An experimental polymer-salt phase diagram for highly charged PDADMAC/PAA samples (pH near 7) is presented in Figure 2. The two-phase (i.e., coacervate) and single-phase samples are indicated by orange circles and green triangles, respectively, and theoretical predictions by solid red lines. This shows, for example, that a sample containing a monomer concentration of 0.15M of each PE and an added salt concentration of 0.15M (NaCl or KCl) undergoes associative phase separation at equilibrium. Samples undergo phase separation at low salt concentration and form a single-phase solution as salt concentration increases to as high as 1.6M. The critical salt concentration for the transition from two phases to one phase, here named the *Upper Critical Salt Concentration (UCSaC)*, is slightly higher for KCl (Figure 2(a)) than for NaCl (Figure 2(b)), which is consistent with Perry and co-workers' report that the stability of the coacervate in addition of sodium ion is weaker than that of the potassium ion. (40) The experimental data in Figure 2 are consistent with the Hofmeister series for cations, where sodium ions bind more strongly to a given

anionic macromolecule than do potassium ions, which could be attributed to lower hydration waters of sodium ions. The theoretical phase boundary or UCSaC, extracted from endpoints of lines at different monomer concentrations in Figure 1(a), is in qualitative agreement with the experimental findings, although it is more accurate at low and medium concentrations. In strong polyelectrolyte complexes, depicted in Figure 1 and 2, the non-electrostatic interaction parameter between PAA and water, χ_{AW} , is set at 0.45, considering water's moderate good solvent for PAA at pH 7.⁽³⁶⁾⁽⁴⁵⁾⁽⁵⁵⁾ It is possible to improve the accuracy of our predictions at high polymer concentrations by adjusting χ_{AW} based on the overall ionic strength in the solution since Flory-Huggins parameter depends not only on temperature but also on the PAA degree of ionization, counterion type and concentration. ⁽⁵⁵⁾

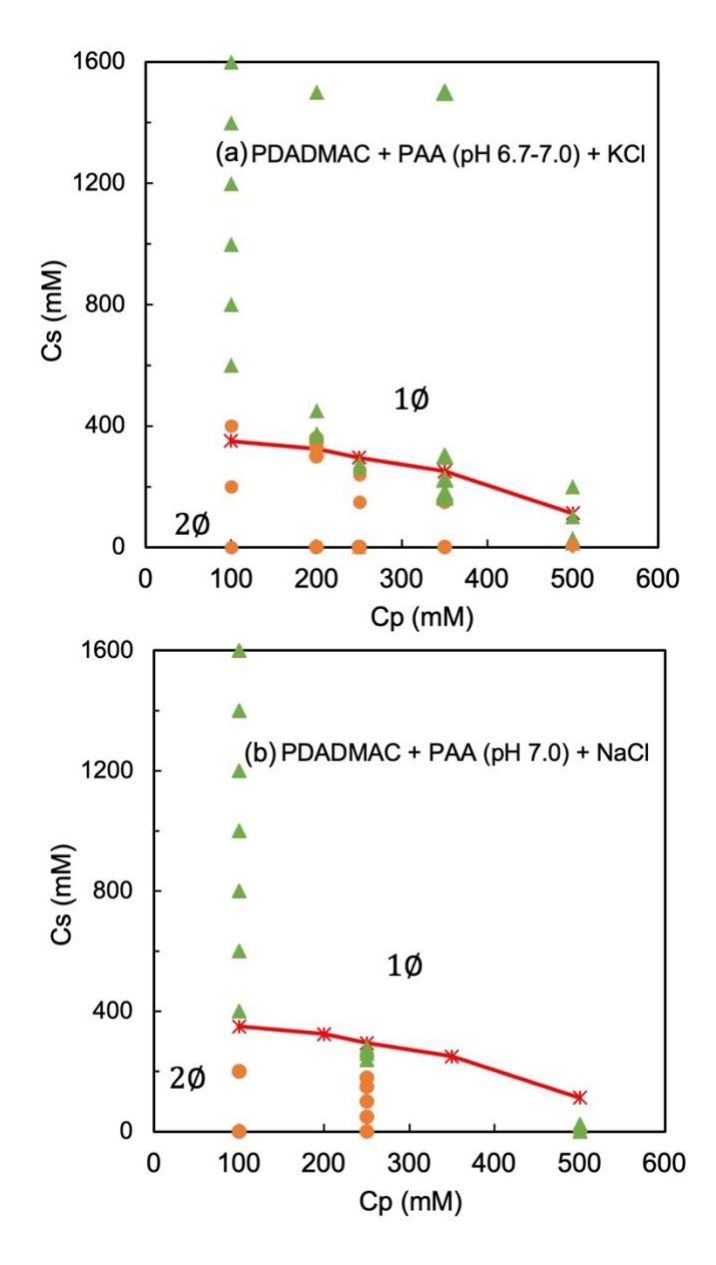


Figure 2. Experimental (symbols) and predicted (lines) phase diagrams of fully (100%) charged PDADMAC/PAA polyelectrolytes with (a) KCl and (b) NaCl. Orange circle and green triangle symbols represent two-phase samples and one-phase solutions, respectively. In this and figures below the axes give the overall monomer concentrations of polymer and of added salt. Here χ_{AW} = 0.45, with other theoretical parameters given in Table 1.

3.2 SEGREGATIVE PHASE SEPARATION

3.2.1 EXPERIMENTAL OBSERVATION OF PHASE RE-ENTRY

In weak polyanions, both undissociated or protonated (neutral) and dissociated or deprotonated (charged) monomers exists along the polymer backbone. While charge on a monomer renders it strongly polar and water soluble, when neutralized, the underlying hydrophobicity of the monomer is exposed, with implications for its interactions with water, salt, and all other species, leading to additional mechanisms for phase separation. In our experiments, when a strong polycation (PDADMA) is mixed in solution with a partially charged polyanion, namely PAA at pH of 5 or 5.2, as salt concentration is increased beyond that needed to dissolve the two-phase solution into a single solution, a re-entrant phase separation occurs, as shown on the phase diagram in Figure 3, and in Figure S2. This shows that salt can both oppose and drive phase separation. Phase diagrams encompassing the high-salt region are shown in Figure 3 for PDADMAC/PAA at two different pH values and two different salts (NaCl and KCl). Low-salt two-phase regions are shown by orange circles, the one phase regions at medium salt by green triangles, and two-phase regions at high salt by blue diamond. Notably, all four systems, for both KCl and NaCl, and at pH 5.0 and 5.2, exhibit phase re-entry in the high salt region. This phase re-entry is also observed at pH 4.7 shown in Figure S3. Typically, phase re-entry occurs at relatively high polymer concentration (above 0.1M for each polymer) and high salt concentration (above 0.8M added salt concentration). Moreover, the higher the polymer concentration, the lower the salt concentration required to trigger the second phase separation. This suggests that a minimum number of monomers per unit volume is required to induce their aggregation at high salt. Comparing Figure 3(a) with 3(c) and 3(b) with 3(d) shows that less KCl is required to drive phase-separation re-entry than is needed with NaCl, for each pH. Thus the single-phase region in KCl is smaller than for NaCl.

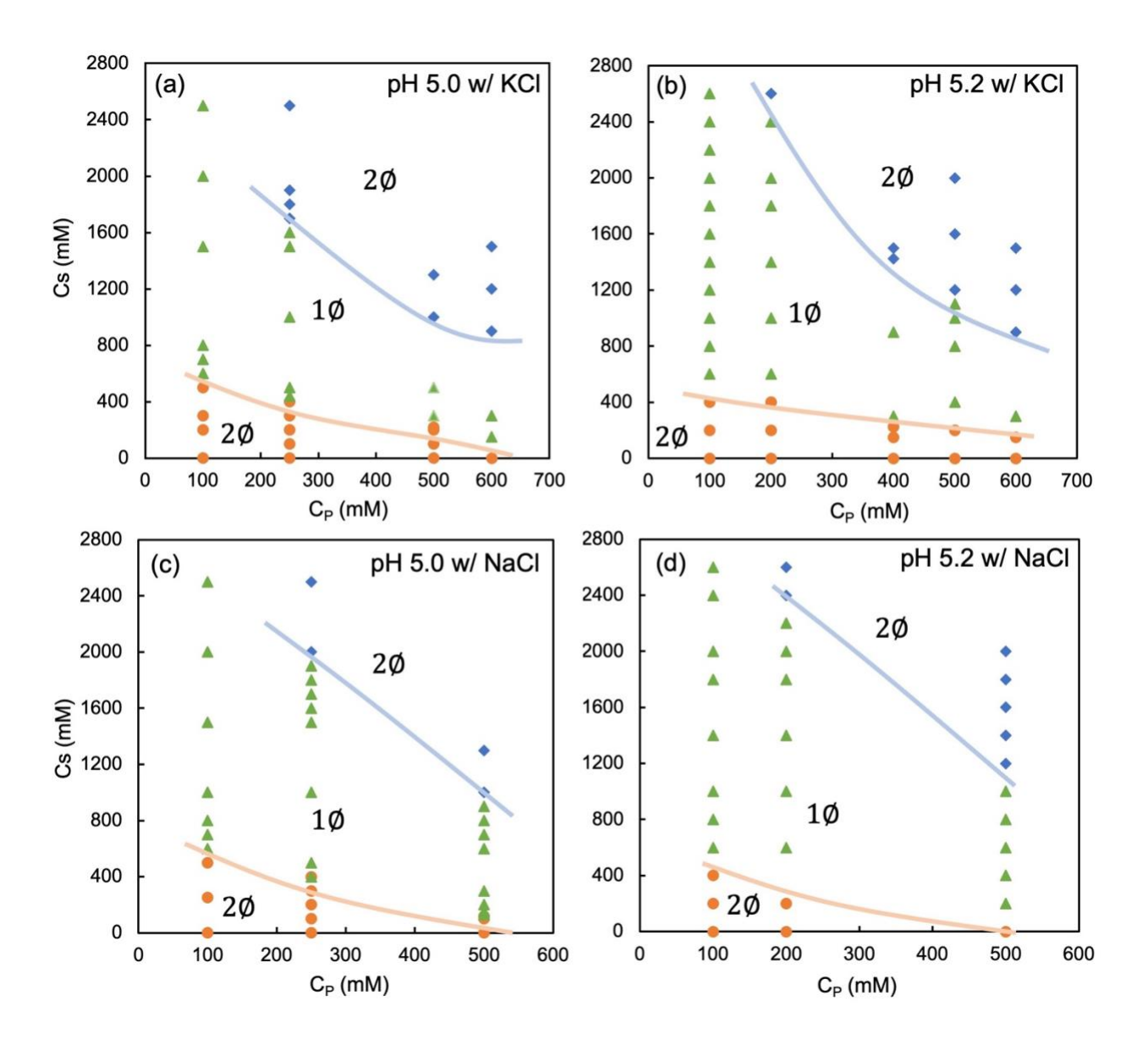


Figure 3. Experimental phase diagrams of weakly charged PDADMAC/PAA polyelectrolyte complexes with (a, b) KCl and (c, d) NaCl at pH (a, c) 5.0 and (b, d) 5.2. Lines are approximations to the phase boundaries based on the experimental points.

Since the two-phase region at low salt in polyelectrolytes is well documented and understood at least qualitatively, it is the surprising re-entrant separation at high salt that is most in need of explanation. A key to the explanation is the observation that *polyacrylic acid (PAA) alone* (in the absence of a polycation) can phase separate upon addition of salt, depending on the degree of

ionization (or equivalently pH), polymer concentration, temperature, salt identity and concentration. (56) This salt-induced phase separation, called "salting out," may be caused by the suppression of hydration of carboxylate groups, thus leading to a more hydrophobic polymer at higher ionic strength. Figure S4 in the SI shows that when the 100 kDa PAA used in Figure 3 is placed in salt solution on its own, without the PDADMAC, at a pH of 5 and a monomer concentration of 0.25 M and 0.5M, it phase-separates at a KCl salt concentrations exceeding 2.4 M or NaCl exceeding 3.0 M. When the PAA is fully charged at pH 7, it does not separate at any accessible salt solution. When polycation is present at the same pH of 5 and monomer concentration of 0.25 M, Figure 3 shows that the phase separation occurs at salt concentrations of 1.6 and 2.0 M, for KCl and NaCl, respectively, well below the values of 2.4 and 3.0 M observed when PDADMA is absent. Thus, the addition of PDADMAC enhances the tendency of PAA to phase separate from water at high salt concentrations.

Thus, the phase re-entry in PDADMAC/PAA solutions is likely caused by the same forces that drive phase separation of weakly charged PAA in the absence of PDADMAC. This would imply that the dense phase formed at high salt concentrations in PDADMAC/PAA solutions should be predominantly PAA, with little PDADMAC. We verified this hypothesis through NMR measurements, whose results are depicted in Figure S5, which demonstrate that PAA is primarily in the denser phase of the phase re-entry sample, while almost all of the PDADMAC remains soluble in the upper, less dense, more liquid-like, phase. Thus, the re-entrant phase separation is segregative, such as is commonly observed in blends of neutral polymers. The composition of a typical associatively phase separated PAA/PDADMAC sample at lower salt is presented in Figure S6, where the majority of both polymers are condensed in the bottom coacervate phase and only

relatively small amount of PDADMAC and virtually no PAA remains in the supernatant phase. This is well understood in associatively separated polymers in which the ratio of charged monomers of the two polyelectrolytes is not too far from unity. For example, it has been reported by Wang et al. that in an associatively separated coacervate phase, consisting of PDADMAC and a strong polyanion, namely poly (styrene sulfonate), the monomer molar ratio of the two polymers is approximately one.⁽⁴⁷⁾

Thus, the transition of $2\emptyset \to 1\emptyset \to 2\emptyset$ shown in Figure 3 with increasing salt concentration represents a shift from associative phase separation to a single solution to segregative phase separation. Associative separation is commonly observed in numerous polyelectrolyte systems with an upper critical salt concentration (UCSaC), whereas segregative separation is much less common, appearing at high salt region and corresponding to a lower critical salt concentration (LCSaC). However, Tirrell and co-workers(44) have reported a segregative phase separation in a system composed of the weak polycation, poly (allylamine hydrochloride) (PAH), and the weak polyanion, PAA, with a PAA to PAH mole ratio of 0.67 in the coacervate under acidic conditions. Our observations here are similar to those in a previous study on anionic polysaccharide sodium hyaluronate (NaHy) and the cationic surfactant tetradecyltrimethylammonium bromide (CTABr), where the addition of NaBr salt (starting from low values) led to: 1) increase of coacervate volume fraction, 2) then dissolution of coacervate and single phase, and 3) finally to a segregative phase separation. (57) This suggests that segregative phase separation is more prevalent in weak polyelectrolytes where the interactions among polyions, water, and salt ions are more polymer specific and non-electrostatic. For example, the ionized carboxylic acid groups (COO-) contribute to the solubility of PAA by interacting electrostatically with dipolar water molecules. However, a high concentration of salt ions Na⁺ or K+ competes with water for the carboxylate ions, reducing the hydration and solubility of the polymer chains, which, along with the hydrophobicity of other parts of the PAA monomer, is likely the source of self-aggregation and precipitation.

3.2.2 THEORETICAL PREDICTIONS

Experimental evidence suggests that the phase re-entry in the PDADMAC/PAA/salt phase diagram may be attributed to the non-electrostatic intermolecular interactions between PAA and water, which can be correlated with the Flory-Huggins parameter, χ_{AW} . To investigate this phenomenon and validate our theoretical assumptions, we used the thermodynamic model outlined in Section 2.2 to calculate the phase behavior of PDADMAC/PAA in salt, varying χ_{AW} for PAA charge levels of 12.5%, 35%, and 100%, at various polymer concentrations. The results in Figure 4 show that the phase re-entry occurs once χ_{AW} exceeds a value that depends on charge level. When $\chi_{AW} = 0.45$, with increasing added salt concentration, all three systems exhibit an increasing volume fraction of coacervate, reaching a single-phase solution at salt concentrations well below 500 mM in all cases, and remaining a single phase up to at least 2000mM added salt. However, for $\chi_{AW} > 0.5$, a second phase separation is induced at high salt concentrations, as evidenced by the re-emergence of v_{dense} between 0 and 1. The value of χ_{AW} needed for the second phase transition increases with PAA charge level, and is around 0.55, 0.62 and 0.75, respectively for 12.5%, 35% and 100% charged PAA. By further increasing the unfavourability of the interaction between PAA and water (i.e., further increasing χ_{AW}), phase separation is observed over the entire range of salt concentration, up to 2000mM, characterized by an initial increase in coacervate volume with increasing salt, a subsequent slight decrease, and an eventual plateau, but with no intervening single-phase region.

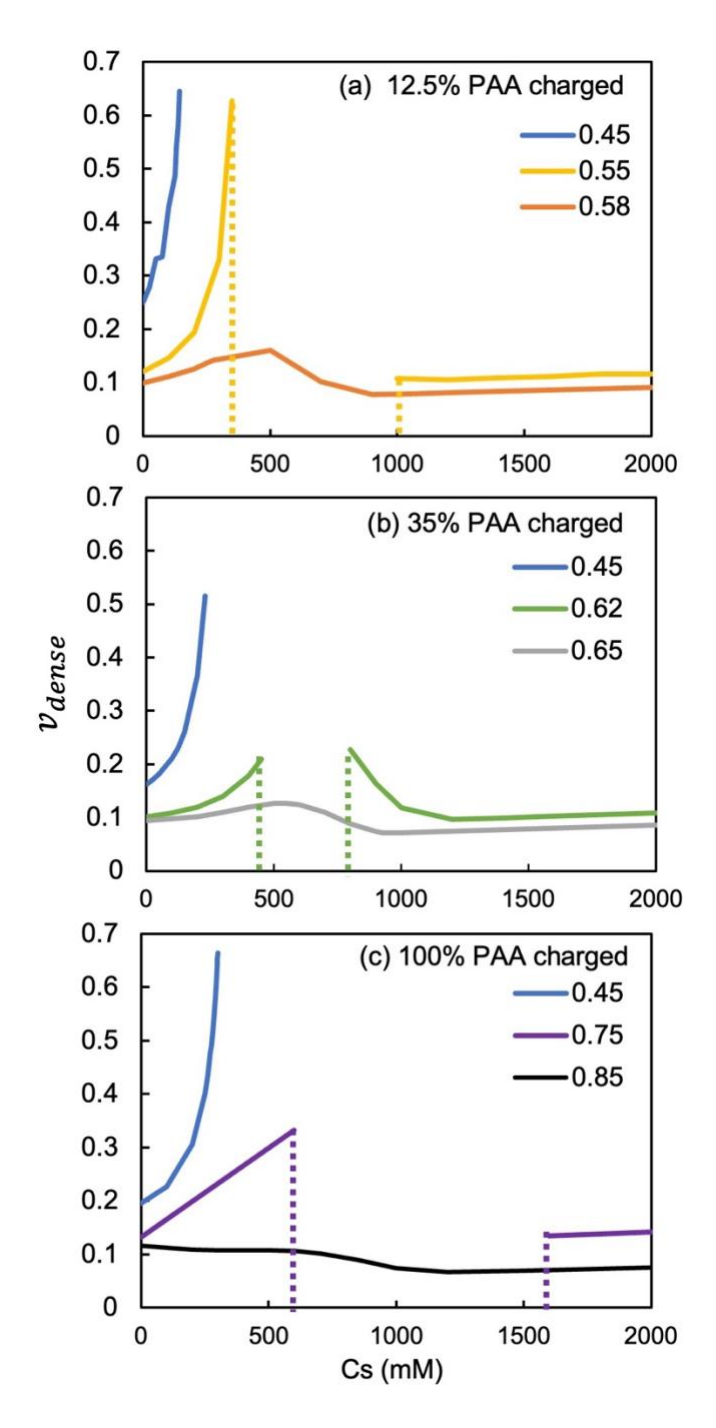


Figure 4. Theoretical volume fraction of separated phase, v_{dense} , as a function of added salt concentration, C_s , for 250 mM monomer concentration of polycation, with PAA charged at: (a) 12.5%, (b) 35%, and (c)100%, for χ_{AW} values in the legend. The polyanion has a charged monomer concentration of (a) 31mM, (b) 88mM, and (c) 250mM, respectively, depending on the

charge level. Additional theoretical input parameters can be found in Table 1. The dashed lines mark the boundaries of the two-phase region, where present.

Figure 5 gives the predicted volume fractions of polycation and polyanion in the dense phase for 12.5% charged PAA. The figure reveals three distinct types of phase transitions. Firstly, at low salt concentration, associative phase separation occurs at χ_{AW} values of 0.45 and 0.50, followed by a decrease in the volume fractions of both polycation and polyanion within the swelling coacervate phase, as salt concentration increases. Secondly, for $\chi_{AW}=0.55$, following the associative separation at low salt concentration, and a single phase at intermediate salt concentration, a phase re-entry due to segregative phase separation is observed at high salt concentrations, with polyanion, but not polycation, in the dense phase. Thirdly, for χ_{AW} values exceeding 0.55, phase separation is observed across the entire range of salt concentration, featuring a gradual transition from an associative to a segregative composition with increasing salt, without the formation of a single-phase solution at intermediate salt concentrations. The first two types of phase transitions were observed in our experiments, in Figure 3. The third type of behavior, without a single-phase region, is absent from our experiments, but was observed by Li et al., who found a two-phase separation in PAA/PAH even at salt concentration up to 4M with a transition from association to segregation when increasing salt concentration under acidic conditions. (44) A open phase boundary or two-phase region was also predicted to exist at very high salt concentrations for PECs in poor solvent by de Pablo and Tirrell's group. (45)

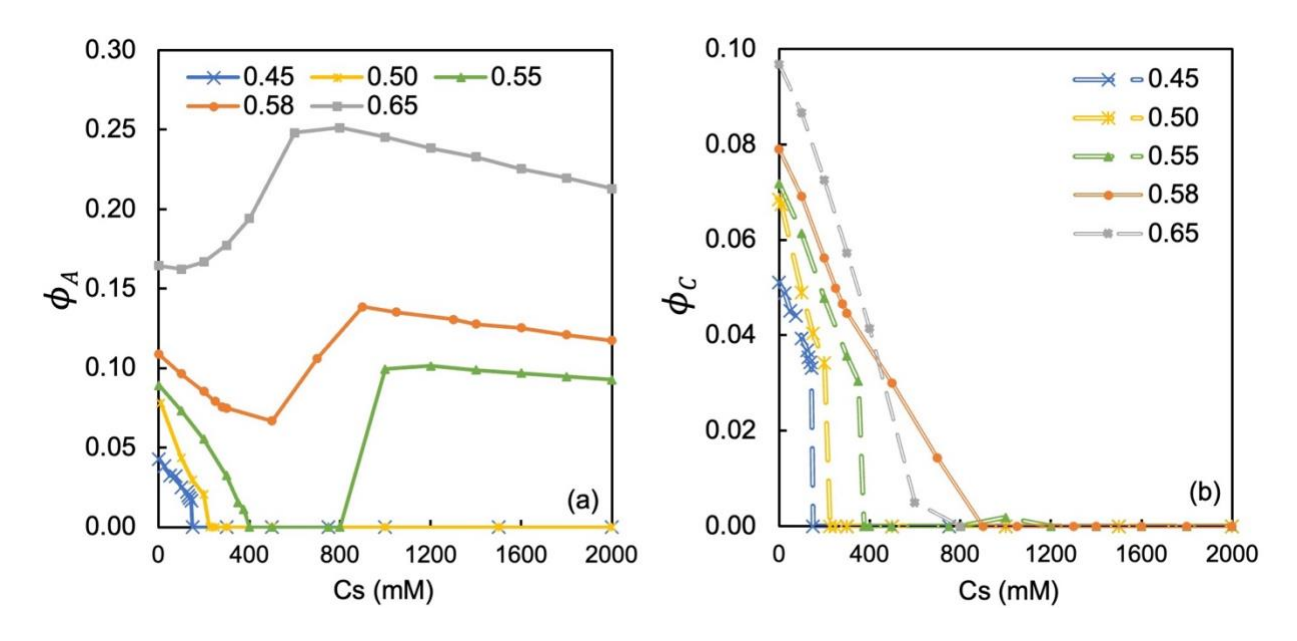


Figure 5. Dependence of the volume fraction of (a) polyanion and (b) polycation in the dense phase on the concentration of added salt, for Flory-Huggins parameter values shown in the legend. Predictions are made for a PAA charge level of 12.5% (i.e., 31mM charged monomer concentration) and polycation monomer concentration of 250mM.

The calculated phase re-entry exhibits sensitivity not only to the charge level of PAA but also to the χ_{AW} value. Figure 6 presents a χ_{AW} -salt phase diagram for 250 mM monomer concentration of each polyion (although charged PAA concentration changes with charge fraction). This "wedge"-shaped diagram contains three regions: orange circles represent associative phase separation, green triangles single phases, and blue diamonds segregative phase separation. Upon increasing χ_{AW} , the single-phase region diminishes in favor of both of the two-phase regions, whether associative or segregative, eventually leading to phase separation across the entire range of salt concentrations. It should be noted that higher PAA charge levels necessitate larger χ_{AW} values to trigger segregative phase separation. For systems containing 12.5%, 35%, and 100% charged PAA, phase re-entry occurs at χ_{AW} values of 0.55, 0.58, and 0.75, respectively, within a

salt concentration of 2000mM. Interestingly, these values are slightly lower than the χ_{AW} required for inducing phase separation of PAA (without polycation) in 2500 mM salt solution, as shown in Figure S7. For PAA solutions (without polycation) with a 250mM monomer concentration and 2500 mM salt, the critical χ_{AW} values for phase separation are approximately 0.58, 0.65, and 0.85 for 12.5%, 35%, and 100% charged PAA, respectively. Thus, in our theory, the presence of 250 mM polycation lowers slightly the critical value of χ_{AW} needed for PAA segregative separation. The simplest explanation for this is that the polycations and their accompanying counterions increases the ionic strength by 10%, thus decreasing the value of χ_{AW} needed for phase separation.

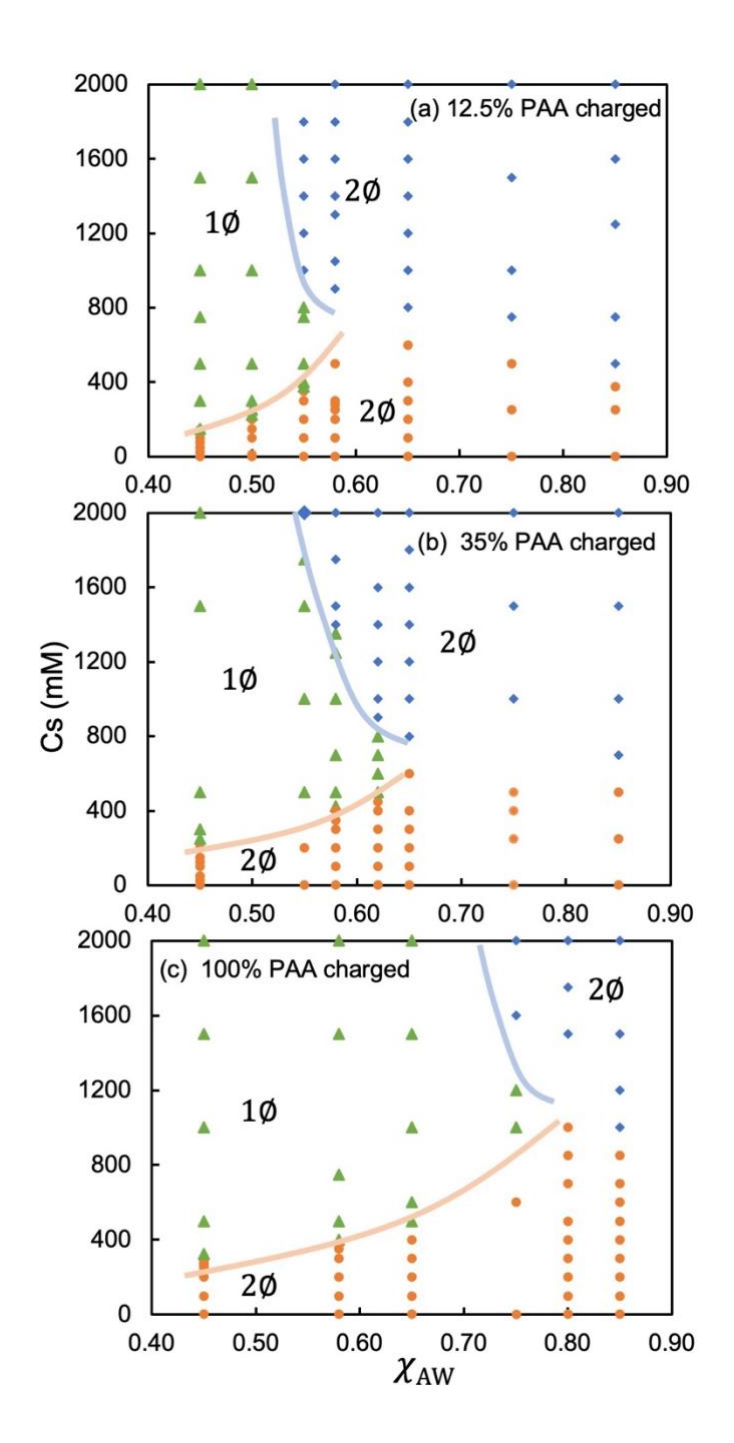


Figure 6. The predicted effect of Flory-Huggins parameter, χ_{AW} , on the phase behavior of partially charged PAA/PDADMAC at polycation monomer concentration 250mM and charged polyanion monomer concentrations 31mM (12.5%), 88mM (35%), and 250mM (100%), with input parameters shown in Table 1. Each symbol is a separate simulation, with associative phase separation (characterized by the existence of both polycation and polyanion), single phase, and

segregative separation (no observations of polycation in the dense phase) represented by orange circles, green triangles, and blue diamonds, respectively.

To compare theory with experiments more directly, theoretical phase diagrams for 12.5% and 35% charged PAA with $\chi_{AW} = 0.55$ and 0.62, respectively, are presented in Figure 7, over polymer concentrations ranging from 100mM to 500mM, with other input parameters again taken from Table 1. Below a polymer concentration of 100mM, no phase re-entry is observed, which is consistent with the experimental findings presented in Figure 3, and indicates that phase re-entry can only be triggered when the polymer concentration exceeds a critical value. Figure 7 also shows a boundary between associative phase separation and a single phase, or so called UCSaC, with negative slope similar to that in experiments in Figure 3. The upper boundaries separating the single-phase region from the segregative phase separation, or LCSaC, however, are predicted by our theory to have a slightly positive slope for PAA system with 12.5% charge and a steeper positive gradient for that with 35% charge, while LCSaC boundaries in the experiments are always negative. Hence, the theory is some distance from being quantitative. This should not be surprising; the parameters in Table 1, and the values of charge fraction on PAA and of χ_{AW} are rough estimates, and both these and the binding free energy ΔG likely depend not only on pH, but on composition, and thus may vary across the phase diagram. Due to the similarity of UCSaC and upper critical solution temperature (UCST) or LCSaC and lower critical solution temperature (LCST), (60) it is reasonable to infer that a relationship between salt and Flory-Huggins parameter could be incorporated into the polyelectrolyte system, analogous to the dependence of χ on temperature in the UCST and LCST phase transitions. Salehi and Larson, (22) for example, showed in a model that contained mass action expressions for protonation reaction equilibrium and water

dissociation (but without the RPA) there were large changes the degree of charge in weak polyelectrolytes, as a function of composition. Thus, the theory presented here is only preliminary, and can be improved by including charge regulation and using experiments and/or MD simulations to obtain better estimates of the parameters for the theory and their dependencies on composition. Despite these substantial limitations, the encouraging qualitative between theory and experiments suggest that the basic physics responsible for both associative and dissociative phase separation in PAA/PDADMAC have been accounted for.

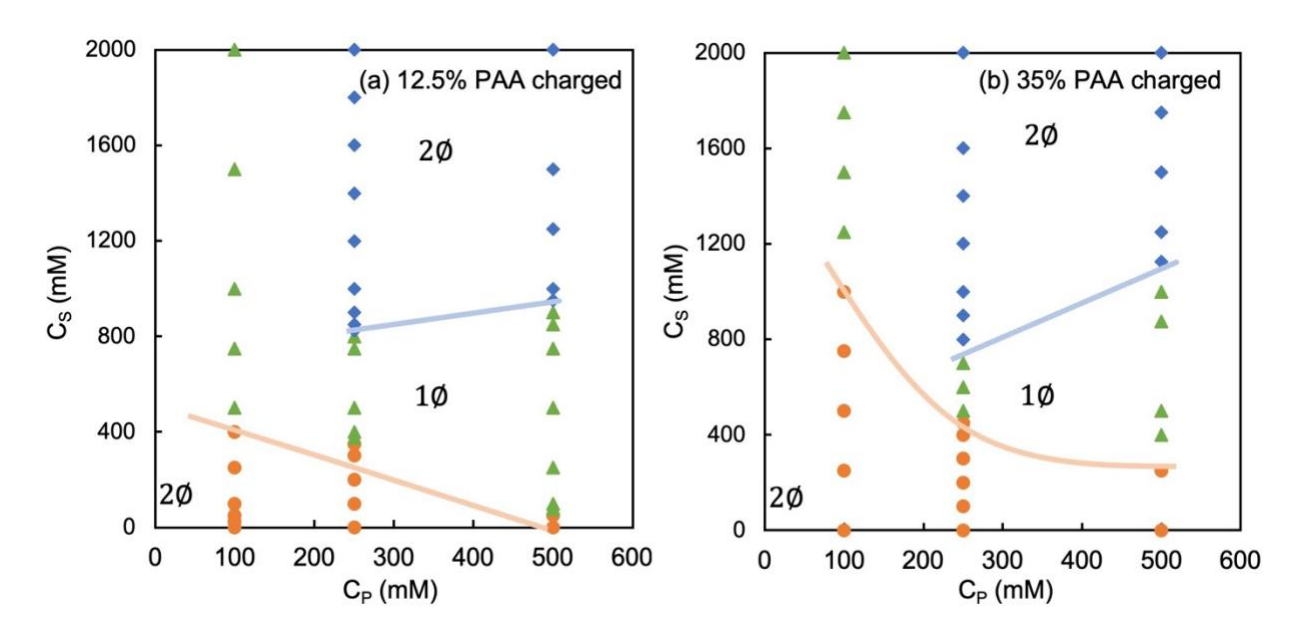


Figure 7. Theoretical polymer-salt phase diagrams of partially charged polyelectrolyte complexes for (a) 12.5% charged PAA with $\chi_{AW} = 0.55$ and (b) 35% charged PAA with $\chi_{AW} = 0.62$. Input parameters can be found in Table 1.

4. CONCLUSIONS

Experimental investigation of the phase behavior of weakly charged polyelectrolyte complexes of PDADMAC/PAA in NaCl and KCl reveal phase-separation re-entry at high salt concentrations, in

which the two polyelectrolytes segregate into different phases. This contrasts with the low-salt associative phase separation and the single-phase region at intermediate salt concentrations. This unique high-salt re-entrant phase separation arises from the segregation of PAA itself, in which the dense phase predominantly contains PAA leaving PDADMAC soluble in the upper supernatant phase, as confirmed by carbon NMR.

Remarkably, this experimental re-entrant segregative phase transition can be fitted semiquantitatively by a thermodynamic theory used previously for low-salt associative phase transitions, by adjusting a single parameter, the Flory-Huggins parameter of the interaction between PAA and water, χ_{AW} . Utilizing our previously developed thermodynamic theory, different values of χ_{AW} lead to the prediction of three different sequences of phase transitions as salt concentration increases. Firstly, for low χ_{AW} < 0.5, an associative phase separation occurs at low salt concentration, with both polymers condensing into the coacervate phase, followed by a single phase at all higher salt concentrations, because of the screening of electrostatic interactions and thus only an upper critical salt concentration (UCSaC) is observed. Secondly, at $\chi_{AW} > 0.5$, and small PAA charge density, or at higher values of both χ_{AW} and charge density, the associative separation and subsequent single-phase region is followed at still higher salt concentrations by a segregative phase-separation re-entry, presumably due to the hydrophobicity of neutral PAA monomers, which drives them into their own PAA-dense phase, separate from the phase containing PDADMAC and excess water. Both the UCSaC and the lower critical salt concentration (LCSaC) are thus present in this case. Thirdly, at higher χ_{AW} , phase separation is predicted to span the entire range from associative to segregative separation, without the intermediate single-phase region or any critical salt concentration. The first two sequences predicted by the theory occur in our

experimental PAA/PDMAC phase diagrams. The third possibility, wherein a gradual salt-induced transition from associative to segregative phase separation occurs without an intervening single-phase region, is predicted but not observed in our experiments, but has been seen in work by Li et al. (44)(45)

By combining experimental observation with theoretical predictions, it can thus be concluded that the equilibrium state in weakly charged polyelectrolyte system is governed by competing driving forces between the electrostatic interactions among charged species and the non-electrostatic interactions, including hydrophobic and hydrogen-bonding interactions induced by un-ionized monomers. The addition of salt ions acts as a potent mediator that can not only facilitate the formation of single solution while also inducing separation within the single solution by the hydrophobic and other interactions among un-ionized polymers. This new finding provides solid evidence, and the beginnings of a quantitative theory, for predicting complex phase behavior involving weak polyelectrolyte systems.

SUPPORTING INFORMATION

Calculations of charge fractions in the literature; Comparisons among experiments, theory with RPA, as well as theory without RPA on strong polyelectrolyte complexes; Experimental phase diagram of weakly charged polyelectrolyte complexes at pH 4.7; The phase separation of single PAA solutions; Carbon NMR spectrum of the associative separation sample and segregative separation sample; Critical χ_{AW} values to make single PAA solution phase separate.

ACKNOWLEDGEMENT

Funding was provided by the National Science Foundation under grants DMR-1707640 and DMR-2100513. Any opinions, findings, and conclusions or recommendations expressed in this material are those of the authors and do not necessarily reflect the views of NSF.

REFERENCES

- (1) Semenova, M. Protein–polysaccharide associative interactions in the design of tailor-made colloidal particles. Curr Opin Colloid In **2017**, 28, 15–21.
- (2) Cubides, T. A. P.; and Amin, S. Surface Activity of Surfactant–Polyelectrolyte Mixtures through Nanoplasmonic Sensing Technology. Cosmet **2022**, 9, 105.
- (3) Chi, K.; and Catchmark, J. M. Improved eco-friendly barrier materials based on crystalline nanocellulose/chitosan/carboxymethyl cellulose polyelectrolyte complexes. Food Hydrocolloid **2018**, 80, 195–205.
- (4) Wilts, E. M.; Herzberger, J.; and Long, T. E. Addressing water scarcity: cationic polyelectrolytes in water treatment and purification. Polym. Int. **2018**, 67, 799–814.
- (5) Muthukumar, M. 50th Anniversary Perspective: A Perspective on Polyelectrolyte Solutions. Macromolecules **2017**, 50 (24), 9528–9560.
- (6) Achazi, K.; Haag, R.; Ballauff, M.; Dernedde, J.; Kizhakkedathu, J. N.; Maysinger, D.; Multhaup, G. Understanding the Interaction of Polyelectrolyte Architectures with Proteins and Biosystems. Angewandte Chemie Int Ed 2021, 60 (8), 3882–3904.
- (7) Overbeek, J. T. G.; and Voorn, M. J. Phase separation in polyelectrolyte solutions. Theory of complex coacervation. Journal of Cellular and Comparative Physiology **1957**, 49, 7-26.
- (8) Flory, P. J. Thermodynamics of high polymer solutions. J. Chem. Phys. **1941**, 9, 660.

- (9) Huggins, M. L. Theory of solutions of high polymers. J. Am. Chem. Soc. **1942**, 64, 7, 1712–1719.
- (10) Debye, P.; and Hückel, E. Z. Theorie der Elektrolyte. Physikalische Zeitschrift, **1923**, 9, 185-206.
- (11) Veis, A. Phase separation in polyelectrolyte solutions II. Interaction effects. J Phys Chem1961, 65, 1798–1803.
- (12) Spruijt, E.; Westphal, A. H.; Borst, J. W.; Stuart, M. A. C.; and van der Gucht, J. Binodal Compositions of Polyelectrolyte Complexes. Macromolecules **2010**, 43, 6476–6484.
- (13) Borue, V. Yu; and Erukhimovich, I. Y.; A statistical theory of weakly charged polyelectrolytes: fluctuations, equation of state and microphase separation.

 Macromolecules 1988, 21, 3240-3249.
- (14) Castelnovo, M.; and Joanny, J. F. Complexation between oppositely charged polyelectrolytes: Beyond the Random Phase Approximation. European Phys J E **2011**, 6, 377–386.
- (15) Kudlay, A.; and Olvera de La Cruz, M. Precipitation of oppositely charged polyelectrolytes in salt solutions. J Chem Phys 2004, 120, 404–412.
- (16) Kudlay, A.; Ermoshkin, A. V.; and Olvera de La Cruz, M. Complexation of oppositely charged polyelectrolytes: effect of ion pair formation. Macromolecules **2004**, 37(24), 9231-9241.
- (17) Friedowitz, S.; Salehi, A.; Larson, R. G.; Qin, J. Role of Electrostatic Correlations in Polyelectrolyte Charge Association. J Chem Phys **2018**, 149 (16), 163335.
- (18) Muthukumar, M., Hua, J., and Kundagrami, A. Charge regularization in phase separating polyelectrolyte solutions. J Chem Phys **2010**, 132, 084901.

- (19) Muthukumar, M. Theory of counter-ion condensation on flexible polyelectrolytes: Adsorption mechanism. J Chem Phys **2004**, 120, 9343–9350.
- (20) Dobrynin, A. V.; and Rubinstein, M. Counterion Condensation and Phase Separation in Solutions of Hydrophobic Polyelectrolytes. Macromolecules **2001**, 34, 1964–1972.
- (21) Tian, W.; Ghasemi, M.; and Larson, R. G. Extracting free energies of counterion binding to polyelectrolytes by molecular dynamics simulations. J Chem Phys **2021**, 155, 114902.
- (22) Salehi, A.; and Larson, R. G. A Molecular Thermodynamic Model of Complexation in Mixtures of Oppositely Charged Polyelectrolytes with Explicit Account of Charge Association/Dissociation. Macromolecules **2016**, 49, 9706–9719.
- (23) Danielsen, S. P. O.; Panyukov, S.; Rubinstein, M. Ion Pairing and the Structure of Gel Coacervates. Macromolecules **2020**, 53 (21), 9420–9442.
- (24) Rumyantsev, A. M.; Johner, A.; Tirrell, M. V.; Pablo, J. J. de. Unifying Weak and Strong Charge Correlations within the Random Phase Approximation: Polyampholytes of Various Sequences. Macromolecules **2022**, 55 (14), 6260–6274.
- (25) Yethiraj, A.; and Shew, C. Y. Structure of polyelectrolyte solutions. Physical review letters **1996**, 77(18), 3937.
- (26) Sing, C. E.; Zwanikken, J. W.; and Olvera de La Cruz, M. Theory of melt polyelectrolyte blends and block copolymers: Phase behavior, surface tension, and microphase periodicity. The Journal of chemical physics 2015, 142(3), 034902.
- (27) Perry, S. L.; and Sing, C. E. Prism-based theory of complex coacervation: Excluded volume versus chain correlation. Macromolecules **2015**, 48(14), 5040-5053.
- (28) Rubinstein, M.; Liao Q.; and Panyukov S. Structure of liquid coacervates formed by oppositely charged polyelectrolytes. Macromolecules **2018**, 51(23), 9572-9588.

- (29) Rumyantsev, A. M.; Zhulina, E. B.; & Borisov, O. V. Complex coacervate of weakly charged polyelectrolytes: Diagram of states. Macromolecules **2018**, 51(10), 3788-3801.
- (30) Rumyantsev, A. M.; & de Pablo, J. J. Liquid crystalline and isotropic coacervates of semiflexible polyanions and flexible polycations. Macromolecules **2019**, 52(14), 5140-5156.
- (31) Wang, Q.; Taniguchi T.; and Fredrickson G. H. Self-consistent field theory of polyelectrolyte systems. The Journal of Physical Chemistry B **2004**, 108(21), 6733-6744.
- (32) Delaney, K. T.; and Fredrickson, G. H. Theory of polyelectrolyte complexation—Complex coacervates are self-coacervates. J Chem Phys **2017**, 146, 224902.
- (33) Muthukumar, M. 50th Anniversary Perspective: A Perspective on Polyelectrolyte Solutions. Macromolecules **2017**, 50 (24), 9528–9560.
- (34) Sing, C. E.; Perry, S. L. Recent Progress in the Science of Complex Coacervation. Soft Matter **2020**, 16 (12), 2885–2914.
- (35) Ghasemi, M.; Larson, R. G. Future Directions in Physiochemical Modeling of the Thermodynamics of Polyelectrolyte Coacervates. AIChe Journal **2022**, 68(5), 17646.
- (36) Ghasemi, M.; Larson, R. G. Role of Electrostatic Interactions in Charge Regulation of Weakly Dissociating Polyacids. Prog Polym Sci **2020**, 112, 101322.
- (37) Ghasemi, M.; Friedowitz, S.; and Larson, R. G. Analysis of Partitioning of Salt through Doping of Polyelectrolyte Complex Coacervates. Macromolecules **2020**, 53, 6928–6945.
- (38) Ghasemi, M.; Friedowitz, S.; and Larson, R. G. Overcharging of polyelectrolyte complexes: an entropic phenomenon. Soft Matter **2020**, 16, 10640–10656.

- (39) Knoerdel, A. R.; McTigue, W. C. B.; Sing, C. E. Transfer Matrix Model of pH Effects in Polymeric Complex Coacervation. J Phys Chem B **2021**, 125 (31), 8965–8980.
- (40) Perry, S. L.; Li, Y.; Priftis, D.; Leon, L.; and Tirrell, M. The Effect of Salt on the Complex Coacervation of Vinyl Polyelectrolytes. Polymers **2014**, 6, 1756–1772.
- (41) Li, L.; Srivastava, S.; Andreev, M.; Marciel, A. B.; de Pablo, J. J.; Tirrell, M. V. Phase Behavior and Salt Partitioning in Polyelectrolyte Complex Coacervates. Macromolecules **2018**, 51 (8), 2988-2995.
- (42) Liu, Y. Structure and Rheology of Polymer Mixtures at the Boundary Between Soft Solid and Viscous Liquid Behaviors From Fundamental Study to Application. University of Michigan. 2021.
- (43) Jha, P. K.; Desai, P. S.; Li, J.; Larson, R. G. pH and Salt Effects on the Associative Phase Separation of Oppositely Charged Polyelectrolytes. Polymers **2014**, 6 (5), 1414–1436.
- (44) Li, L.; Srivastava, S.; Meng, S.; Ting, J. M.; and Tirrell, M. V. Effects of Non-Electrostatic Intermolecular Interactions on the Phase Behavior of pH-Sensitive Polyelectrolyte Complexes. Macromolecules **2020**, 53, 7835–7844.
- (45) Li, L.; Rumyantsev, A. M.; Srivastava, S.; Meng, S.; de Pablo, J. J.; Tirrell, M. V. Effect of Solvent Quality on the Phase Behavior of Polyelectrolyte Complexes. Macromolecules **2021**, 54, 105-114.
- (46) Johnston, A. R.; Perry, S. L.; Ayzner, A. L. Associative Phase Separation of Aqueous π-Conjugated Polyelectrolytes Couples Photophysical and Mechanical Properties. Chem Mater 2021, 33(4), 1116-1129.
- (47) Wang, Q.; Schlenoff, J. B. The Polyelectrolyte Complex/Coacervate Continuum.

 Macromolecules **2014**, 47 (9), 3108–3116.

- (48) Lee, M.; Perry, S. L.; Hayward, R. C. Complex Coacervation of Polymerized Ionic Liquids in Non-Aqueous Solvents. Acs Polym Au **2021**, 1 (2), 100–106.
- (49) Larson, R. G.; Liu, Y.; Li, H. Linear Viscoelasticity and Time-Temperature-Salt and Other Superpositions in Polyelectrolyte Coacervates. Journal of Rheology **2021**, 65 (1), 77–102.
- (50) Li, H.; Liu, Y.; Shetty, A.; Larson, R. Low-Frequency Elastic Plateau in Linear Viscoelasticity of Polyelectrolyte Coacervates. Journal of Rheology **2022**, 66,1067-1077.
- (51) Colby, R. H.; and Rubinstein, M. Polymer physics. New-York: Oxford University 2003.
- (52) Akkaoui, K.; Yang, M.; Digby, Z. A.; Schlenoff, J. B. Ultraviscosity in Entangled Polyelectrolyte Complexes and Coacervates. Macromolecules **2020**, 53 (11), 4234–4246.
- (53) Hyman, A. A.; Weber, C. A.; Jülicher, F. Liquid-Liquid Phase Separation in Biology. Annu. Rev. Cell Dev. Biol. **2014**, 30 (1), 39–58
- (54) Spruijt, E. Open Questions on Liquid–Liquid Phase Separation. Commun Chem **2023**, 6 (1), 23.
- (55) Safronov, A. P.; Adamova, L. V.; Blokhina, A. S.; Kamalov, I. A.; Shabadrov, P. A. Flory-Huggins Parameters for Weakly Crosslinked Hydrogels of Poly(Acrylic Acid) and Poly(Methacrylic Acid) with Various Degrees of Ionization. Polym. Sci. Ser. A 2015, 57 (1), 33–42.
- (56) Ikegami, A.; & Imai, N. Precipitation of polyelectrolytes by salts. Journal of polymer science, **1962**, 56(163), 133-152.
- (57) Thalberg, K.; Lindman, B.; & Karlstroem, G. Phase behavior of a system of cationic surfactant and anionic polyelectrolyte: the effect of salt. The Journal of Physical Chemistry **1991**, 95(15), 6004-6011.

- (58) Ye, Z.; Sun, S.; Wu, P. Distinct Cation–Anion Interactions in the UCST and LCST Behavior of Polyelectrolyte Complex Aqueous Solutions. Acs Macro Lett **2020**, 9 (7), 974–979.
- (59) Litmanovich, E. A.; Chernikova, E. V.; Stoychev, G. V.; Zakharchenko, S. O. Unusual Phase Behavior of the Mixture of Poly(Acrylic Acid) and Poly(Diallyldimethylammonium Chloride) in Acidic Media. Macromolecules **2010**, 43 (16), 6871–6876.
- (60) Adhikari, S.; Prabhu, V. M.; Muthukumar, M. Lower Critical Solution Temperature Behavior in Polyelectrolyte Complex Coacervates. Macromolecules **2019**, 52 (18), 6998–7004.